Influence of Carrier-Based PWM Techniques on the Common-Mode Voltage and Common-Mode Current of Six-Phase Full-Bridge Inverters

Juris Arrozy, Esin Ilhan Caarls, Henk Huisman, Jorge L. Duarte, Lorenzo Ceccarelli
Eindhoven University of Technology
5612AZ Eindhoven
Eindhoven, The Netherlands
Email: j.arrozy@tue.nl

Keywords

≪Pulse Width Modulation (PWM)≫, ≪EMC/EMI≫, ≪Leakage current≫, ≪Multiphase drive≫, ≪Open-end windings≫

Abstract

This paper compares several carrier-based PWM techniques to see their impact on the common-mode voltage (CMV) and common-mode current (CMC) of a six-phase full-bridge inverters. Fast Fourier Transform (FFT) analysis displays the dominant harmonics spectrum of each carrier-based PWM technique. The influence of dead-time on the CMV and CMC is also addressed. Simulation and experimental results are included.

Introduction

Multiphase machine drives have recently gained attention because of their potential candidacy in various propulsion applications such as electric vehicles, electric ship propulsion, and more-electric aircraft [1, 2]. This is mainly because of their advantages such as higher torque density [3], better fault-tolerant operation [4], and reduced input current ripple [5]. For this reason, many aspects of multiphase machine drives such as modelling, control, and modulation techniques has received much attention [2, 6, 7].

The open-winding multiphase machine offers a variant to the traditional wye/delta configuration. This yields better dc voltage utilization at the cost of doubled switch count [8]. This also allows more flexibility in the selection of modulation techniques such as space-vector modulation [9] and carrier-based PWM techniques [10].

Carrier-based PWM techniques are considered to be more suited to multiphase machine drive applications because of their simplicity [10]. There are already several papers that address the influence of carrier-based PWM techniques on the input current ripple [11] and output voltage and current total harmonic distortion (THD) performance [12] in the context of open-winding machine drives. However, the influence of carrier-based PWM techniques on the common-mode voltage (CMV) and common-mode current (CMC) of the motor-inverter system have not been thoroughly addressed yet. This is especially important because the CMV and CMC generated in the machine can lead to EMI-related problems such as bearing degradation and high-frequency noise.

Therefore, this paper compares the influence of several carrier-based PWM techniques on the CMV and CMC performance of the open-winding machine drive. The case study chosen here is a six-phase full-bridge inverter supplying a six-phase open-winding permanent magnet synchronous motor (PMSM). Several carrier-based PWM techniques are considered, namely unipolar modulation, phase-shifted PWM (PS-PWM), and level-shifted PWM (LS-PWM) for the cases of double three-phase and symmetrical six-phase systems. Fast Fourier Transform (FFT) is used to inspect the dominant harmonics spectrum of the

CMV and CMC. The influence of dead-time is also addressed. Simulation and experimental results are included to see which carrier-based PWM techniques generate the highest rms value of common-mode current to the six-phase full-bridge inverters.

CMV and CMC of Six-Phase Full-Bridge Inverters

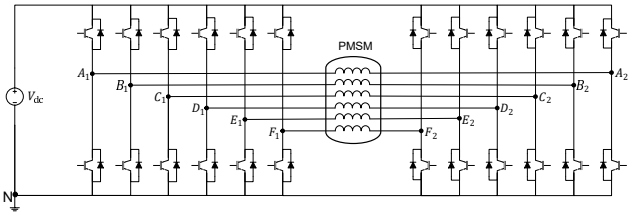

Fig. 1: Six-phase full-bridge inverter supplying a six-phase PMSM

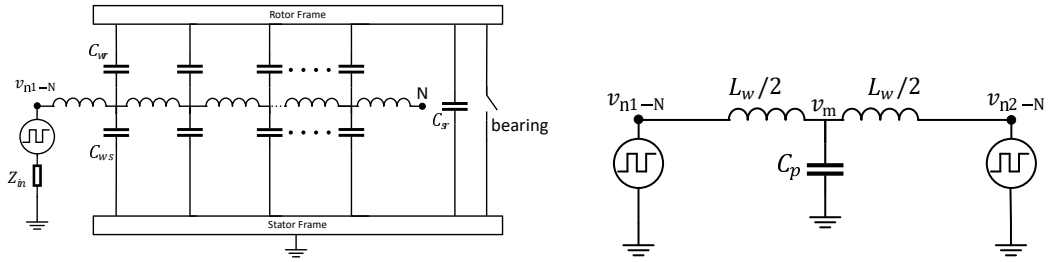

(a) Extended model (b) T-model

Fig. 2: Single winding high-frequency-EM model for the CMC path

Fig. 1 shows a six-phase full-bridge inverters supplying a six-phase open-winding PMSM. When the inverters legs are switching, a rapid change of voltage in the voltage node occurs. This causes a leakage current via the machine's parasitic capacitance, which leads to EMI-related problems such as bearing degradation and high-frequency noise.

There are several ways to model the leakage current path. One of them is the extended model, which models the parasitic capacitance between winding-rotor (C_{wr}), winding-stator (C_{ws}), and rotor-stator (C_g), in addition to the bearing that is modeled as a switch [13]. The extended model is shown in Fig. 2a.

Since the interest of this paper is just to see the influence of carrier-based PWM techniques on the CMV and CMC of the six-phase full-bridge inverters, the extended model is not favourable for it complicates the circuit beyond necessity. Thus, the T-model as in Fig. 2b is proposed as a simplification of the extended model. The leakage current path is provided by the parasitic capacitance (C_p) from the winding to the ground (i.e. housing of the PMSM). In this model, the square-wave input voltage is applied. The leakage current depends on the change of the midpoint voltage of the winding. The steady-state midpoint voltage (v_{m}) of a winding is given as

$$v_{\mathrm{m}} = \frac{v_{\mathrm{n1\text{-}N}} + v_{\mathrm{n2\text{-}N}}}{2} \tag{1}$$

Taking (1) into account, the CMV of six-phase full-bridge inverter is formulated as

$$v_{\mathrm{cm}} = \frac{1}{6} \sum_{n=A\ldots F} \frac{v_{\mathrm{n1\text{-}N}} + v_{\mathrm{n2\text{-}N}}}{2} \tag{2}$$

Ignoring the influence of L_w, the CMC of the six-phase full-bridge inverter is approximated as

$$i_{\mathrm{cm}} = C_p \frac{d}{dt} \left(\sum_{n=A\ldots F} \frac{v_{\mathrm{n1\text{-}N}} + v_{\mathrm{n2\text{-}N}}}{2} \right) \tag{3}$$

It follows from (2) and (3) that to minimize the CMC, v_{cm} should remain as constant as possible with minimum level jumps. This depends on the switching sequence of each H-bridge, which in its turn depends on the carrier-based PWM technique used.

Carrier-Based PWM Techniques

Four carrier-based PWM techniques are considered in this paper: bipolar modulation, unipolar modulation, phase-shifted PWM (PS-PWM), and level-shifted PWM (LS-PWM). In addition, double three-phase and symmetrical six-phase systems are considered. These are shown in Fig. 3 and Fig. 4, respectively.

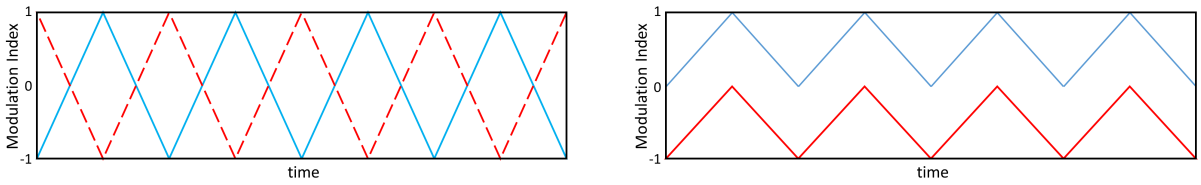

Fig. 3: Carrier Signal for: Phase-shifted PWM / PS-PWM (left) and Level-shifted PWM / LS-PWM (right)

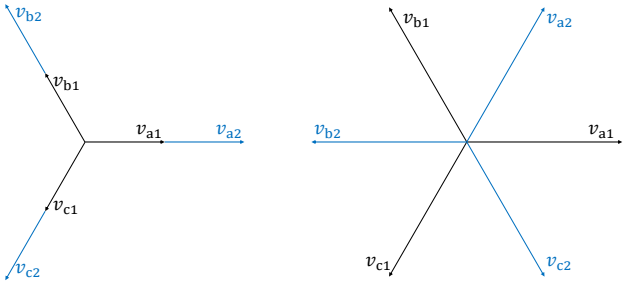

Fig. 4: Double three-phase (left) and symmetrical six-phase systems (right)

Since in bipolar modulation and PS-PWM v_{m} is always half of the dc link voltage (V_{dc}), the CMV is always constant and hence the CMC produced will be theoretically zero. For unipolar and level-shifted modulation, there are cases when both of the high-side switches in an H-bridge are on, making $v_{\mathrm{m}} = V_{\mathrm{dc}}$. Thus, there will be CMC induced because of the voltage change. For a double three-phase system, v_{m} over a carrier period for unipolar modulation and LS-PWM is depicted in Fig. 5.

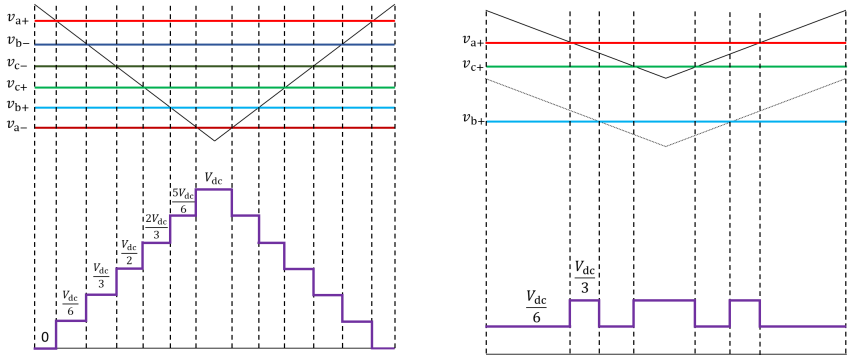

Fig. 5: Example of midpoint voltage (v_{m}) over a carrier period in an H-bridge for: unipolar modulation (left) and LS-PWM (right)

Simulation Results

Table I: System parameters for six-phase full-bridge inverter

Parameters	Value
V_{dc}	400V
R_w	1Ω
L_w	4mH
R_{damp}	600Ω
C_p	4.5nF
f_s	20kHz
m	0.7

Table I shows the system parameters of the six-phase full-bridge inverters and the motor. Each winding is modeled as an inductance (L_w), a resistance (R_w), and a leakage capacitance in the center of the winding to the housing (C_p). A damping resistance (R_{damp}) is included in series with the C_p to model the skin effect of the winding resistance so that the oscillation due to the series connection of L_w and C_p is damped. For the test case of f_s=20kHz and m=0.7, the results are shown in Fig. 6, Fig. 7, and Table II:

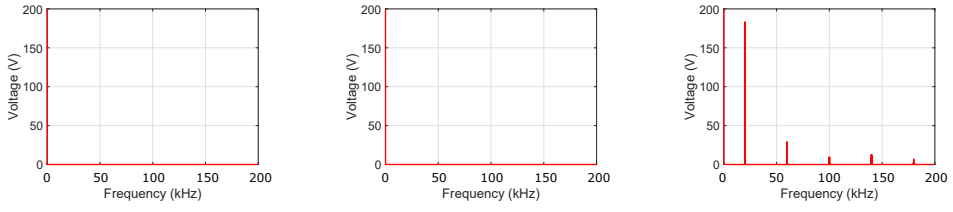

(a) Bipolar modulation (2x3p & 6p)

(b) PS-PWM (2x3p & 6p)

(c) Unipolar Modulation (2x3p)

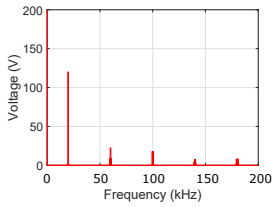

(d) Unipolar Modulation (6p)

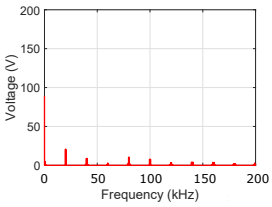

(e) LS-PWM (2x3p)

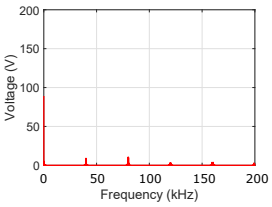

(f) LS-PWM (6p)

Fig. 6: CMV of six-phase full-bridge inverter for various carrier-based PWM techniques

Table II: RMS value of the CMC of six-phase full-bridge inverters for various modulations

	CMC (Arms)	
	2x3p	6p
Bipolar	0	0
PS-PWM	0	0
Unipolar	0.807	0.744
LS-PWM	1.269	1.243

As shown in Fig. 6a, the bipolar modulation and LS-PWM result in a constant CMV of 200V (half of V_{dc}). This is because in bipolar modulation and LS-PWM the midpoint voltage (v_{m}) is always $V_{\text{dc}}/2$ due to the complementary switching pattern of the two legs in an H-bridge. As a result, there is no CMC induced in such modulation techniques (see Fig. 7a).

It is shown in Fig. 6c & Fig. 6d that odd harmonics occur in the CMV of the inverter for unipolar modulation. This is because the resulting CMV waveform meets the requirement of odd and half-wave

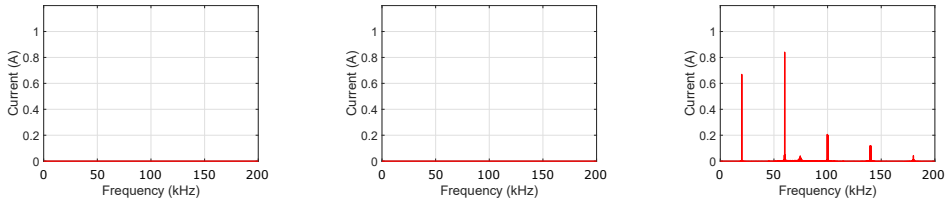

(a) Bipolar modulation (2x3p & 6p)

(b) PS-PWM (2x3p & 6p)

(c) Unipolar Modulation (2x3p)

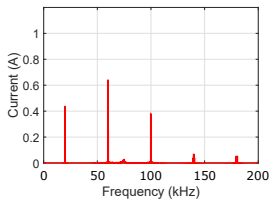

(d) Unipolar Modulation (6p)

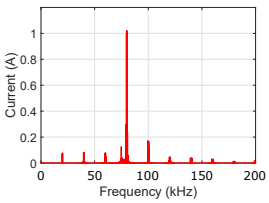

(e) LS-PWM (2x3p)

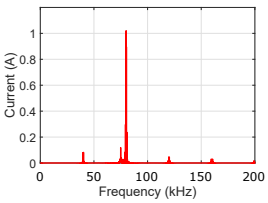

(f) LS-PWM (6p)

Fig. 7: CMV of six-phase full-bridge inverter for various carrier-based PWM techniques

symmetry, as indicated in Fig. 5 (left).

In the case of LS-PWM, different harmonics occur depending on the current phasors of the six-phase system. For the double three-phase system (Fig. 6e), the fundamental frequency of the CMV is the switching frequency. Since the CMV waveform does not meet the requirements of half-wave symmetry, both odd and even harmonics occur in the FFT result. For the symmetrical six-phase system (Fig. 6d), only even harmonics appear in the FFT spectrum. This is because of the combination of v_{m} produced by two opposing phases, which results in CMV with the first harmonic being twice the switching frequency. Therefore, the spectrum are the twofold multiplication of the original spectrum in Fig. 6e.

For the CMC spectrum in unipolar modulation and LS-PWM, it is shown that the 80kHz component shows the highest amplitude of CMC. This is because 80kHz is close to the resonance frequency between the parallel connection of two $\frac{L_w}{2}$ and C_p. It is shown in Table II that double three-phase LS-PWM yields the highest rms value of CMC out of all PWM tecnhiques. This is because in double three-phase LS-PWM all the odd and even harmonics appear, which adds up to the total rms value of CMC in the six-phase full-bridge inverters. Another reason is because in LS-PWM, 80kHz frequency appears in the harmonic spectrum of the CMV, which induces higher CMC to the circuit.

Influence of Dead-time on Bipolar Modulation and PS-PWM

The dead-time of 2μs is added to the circuit to see its influence on the bipolar modulation and PS-PWM. The results are shown in Fig. 8, Fig. 9, and Table III.

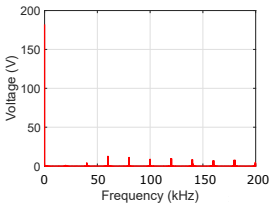

(a) Bipolar modulation (2x3p)

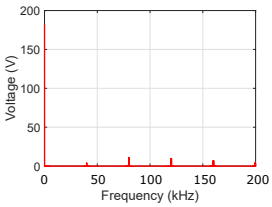

(b) Bipolar modulation (6p)

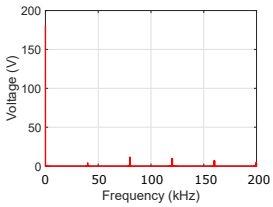

(c) PS-PWM (2x3p)

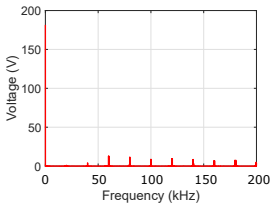

(d) PS-PWM (6p)

Fig. 8: CMV of six-phase full-bridge inverter for bipolar modulation and PS-PWM considering the effect of dead-time

From the results above, it is shown that introducing dead-time causes the bipolar modulation and PS-PWM to have considerable CMV and CMC. This is because the dead-time makes the v_{m} in an H-bridge

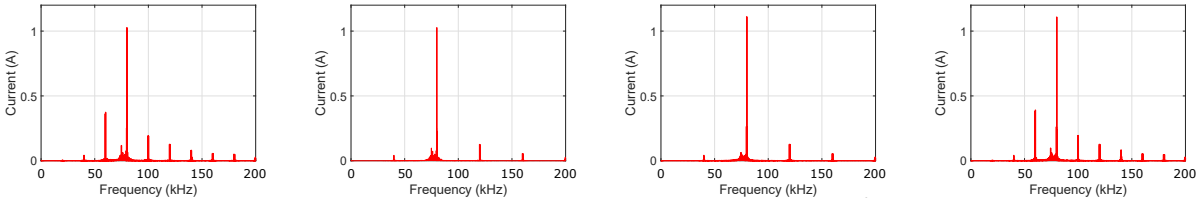

(a) Bipolar modulation (2x3p) (b) Bipolar modulation (6p) (c) PS-PWM (2x3p) (d) PS-PWM (6p)

Fig. 9: CMC of six-phase full-bridge inverter for bipolar modulation and PS-PWM considering the effect of dead-time

Table III: RMS value of the CMC of six-phase full-bridge inverters for various modulations

	CMC (Arms)	
	2x3p	6p
Bipolar	0.916	0.801
PS-PWM	0.801	0.916

equal to zero when all the switches are turned off. This introduces dv/dt, which in turn induces CMC in the circuit. Additionally, it is also shown that the CMV and CMC results between bipolar modulation double three-phase and PS-PWM symmetrical six-phase (and those of bipolar modulation symmetrical six-phase and PS-PWM double three-phase) are similar. This is because the 180° phase-shifted carrier causes the double three-phase system to behave like a symmetrical six-phase system and vice versa.

Experimental Results

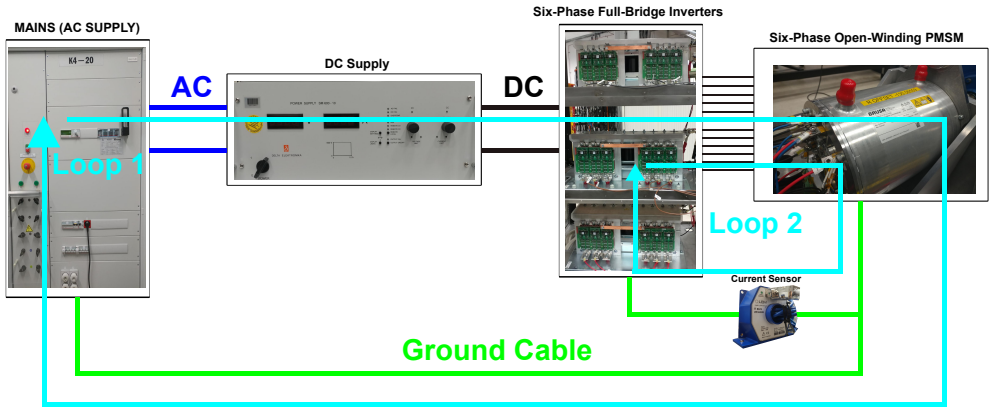

Fig. 10: Experimental Setup for the CMC measurement of Six-Phase Full-Bridge Inverters

Table IV: System parameters for six-phase full-bridge inverter

Parameters	Value
V_{dc}	100V
R_w	0.2Ω
L_w	4mH
C_p	4.5nF
f_s	20kHz
m	0.7
dead-time	2μs

Table V: RMS value of the CMC of six-phase full-bridge inverters for various modulations (experimental results)

	CMC (Arms)	
	2x3p	6p
Bipolar	0.077	0.063
PS-PWM	0.049	0.023
Unipolar	0.086	0.078
LS-PWM	0.1	0.073

Fig. 10 and Table IV show the system parameters for the experimental setup of six-phase full-bridge inverters. It is shown in Fig. 10 that the CMC measurement takes place in the ground cable connecting the PMSM housing and frame and heatsink of the inverter. The CMC loop (see loop 1 in Fig. 10) consists of the motor housing, frame and heatsink of the inverter, and go back to the machine via the cable connection. The second CMC path (loop 1 in Fig. 10) via the mains to the inverter via the DC source is ignored here because 1) the loop is bigger than loop 2; 2) the DC supply is an isolated one.

Table V shows the experimental results for the CMC measurement of six-phase full-bridge inverters for various carrier-based PWM techniques. It is shown that the double three-phase LS-PWM yields the highest rms value of CMC, as also shown in the simulation results. In addition, it is shown that bipolar modulation and PS-PWM also yield a considerable amount of CMC. This is mainly caused by the presence of dead-time in the experimental setup.

Conclusion

This paper compares several carrier-based PWM techniques to see their effect on the CMV and CMC of a six-phase full-bridge inverters. The CMV and CMC of the inverters is important because it can lead to EMI-related problems such as bearing degradation and high-frequency noise. In the given test bench, simulation and experimental results show that double three-phase LS-PWM yields the highest rms value of CMC on the six-phase full-bridge inverters. This is because in double three-phase LS-PWM all the odd and even harmonics spectrum appear in the CMC, which adds up to the total rms value. Bipolar modulation and PS-PWM does not induce CMC on the inverter circuit because the midpoint voltage is always half of the dc-link voltage. However, the inclusion of dead-time in the circuit causes both bipolar modulation and PS-PWM to generate CMC to the inverter circuit.

For future research, the CMV and CMC model will be included with the influence of switches parasitic capacitance, switching transient, and propagation delay. This will yield more accurate CMV and CMC estimation of the six-phase full-bridge inverters.

References

[1] E. Levi, "Multiphase Electric Machines for Variable-Speed Applications," in *IEEE Transactions on Industrial Electronics*, vol. 55, no. 5, pp. 1893-1909, May 2008, doi: 10.1109/TIE.2008.918488.

[2] E. Levi, "Advances in Converter Control and Innovative Exploitation of Additional Degrees of Freedom for Multiphase Machines," in *IEEE Transactions on Industrial Electronics*, vol. 63, no. 1, pp. 433-448, Jan. 2016, doi: 10.1109/TIE.2015.2434999.

[3] K. Wang, Z. Q. Zhu and G. Ombach, "Torque Improvement of Five-Phase Surface-Mounted Permanent Magnet Machine Using Third-Order Harmonic," in *IEEE Transactions on Energy Conversion*, vol. 29, no. 3, pp. 735-747, Sept. 2014, doi: 10.1109/TEC.2014.2326521.

[4] J. Arrozy, D. V. Retianza, J. L. Duarte and H. Huisman, "Fault-Tolerant Control of Series Connectable Modular Full-Bridge Inverter Mitigating Open Switch Faults," *2020 22nd European Conference on Power Electronics and Applications (EPE'20 ECCE Europe)*, 2020, pp. P.1-P.9, doi: 10.23919/EPE20ECCEEurope43536.2020.9215820.

[5] L. Jin, S. Norrga, H. Zhang and O. Wallmark, "Evaluation of a multiphase drive system in EV and HEV applications," *2015 IEEE International Electric Machines & Drives Conference (IEMDC)*, 2015, pp. 941-945, doi: 10.1109/IEMDC.2015.7409174.

[6] F. Barrero and M. J. Duran, "Recent Advances in the Design, Modeling, and Control of Multiphase Machines—Part I," in *IEEE Transactions on Industrial Electronics*, vol. 63, no. 1, pp. 449-458, Jan. 2016, doi: 10.1109/TIE.2015.2447733.

[7] M. J. Duran and F. Barrero, "Recent Advances in the Design, Modeling, and Control of Multiphase Machines—Part II," in *IEEE Transactions on Industrial Electronics*, vol. 63, no. 1, pp. 459-468, Jan. 2016, doi: 10.1109/TIE.2015.2448211.

[8] Z. Liu, Y. Li and Z. Zheng, "A review of drive techniques for multiphase machines," in *CES Transactions on Electrical Machines and Systems*, vol. 2, no. 2, pp. 243-251, June 2018, doi: 10.30941/CESTEMS.2018.00030.

[9] E. Levi, I. N. W. Satiawan, N. Bodo and M. Jones, "A Space-Vector Modulation Scheme for Multilevel Open-End Winding Five-Phase Drives," in *IEEE Transactions on Energy Conversion*, vol. 27, no. 1, pp. 1-10, March 2012, doi: 10.1109/TEC.2011.2178074.

[10] N. Bodo, E. Levi and M. Jones, "Investigation of Carrier-Based PWM Techniques for a Five-Phase Open-End Winding Drive Topology," in *IEEE Transactions on Industrial Electronics*, vol. 60, no. 5, pp. 2054-2065, May 2013, doi: 10.1109/TIE.2012.2196013.

[11] J. Arrozy, H. Huisman and J. L. Duarte, "Input Current Ripple Analysis of Six-Phase Full-Bridge Inverters," *2021 IEEE 12th Energy Conversion Congress Exposition - Asia (ECCE-Asia)*, 2021, pp. 131-136, doi: 10.1109/ECCE-Asia49820.2021.9479174.

[12] F. Patkar, A. Jidin, E. Levi and M. Jones, "Performance comparison of symmetrical and asymmetrical six-phase open-end winding drives with carrier-based PWM," *2017 6th International Conference on Electrical Engineering and Informatics (ICEEI)*, 2017, pp. 1-6, doi: 10.1109/ICEEI.2017.8312446.

[13] Shaotang Chen, T. A. Lipo and D. Fitzgerald, "Modeling of motor bearing currents in PWM inverter drives," *IAS '95. Conference Record of the 1995 IEEE Industry Applications Conference Thirtieth IAS Annual Meeting*, 1995, pp. 388-393 vol.1, doi: 10.1109/IAS.1995.530326.

[14] A. Boglietti, A. Cavagnino and M. Lazzari, "Experimental High-Frequency Parameter Identification of AC Electrical Motors," in *IEEE Transactions on Industry Applications*, vol. 43, no. 1, pp. 23-29, Jan.-feb. 2007, doi: 10.1109/TIA.2006.887313.

[15] A. Boglietti, E. Carpaneto (2001) An Accurate Induction Motor High-Frequency Model for Electromagnetic Compatibility Analysis, *Electric Power Components and Systems*, 29:3, 191-209, DOI: 10.1080/153250001300006626